JOURNAL OF COLLOID AND INTERFACE SCIENCE **179,** 57–65 (1996)
ARTICLE NO. 0188

Kinetics of Interfacial Tension Changes during Protein Adsorption from Sessile Droplets on FEP–Teflon

WIESJE VAN DER VEGT,* WILLEM NORDE,† HENNY C. VAN DER MEI,* AND HENK J. BUSSCHER*,[1]

*Laboratory for Materia Technica, University of Groningen, Bloemsingel 10, 9712 KZ Groningen, The Netherlands; and †Department of Physical and Colloid Chemistry, Wageningen Agricultural University, Dreijenplein 6, 6703 HB Wageningen, The Netherlands

Received March 20, 1995; accepted October 25, 1995

Interfacial tension changes during protein adsorption at both the solid–liquid and the liquid–vapor interface were measured simultaneously by ADSA-P from sessile solution droplets on FEP–Teflon. Two large proteins (albumin and immunoglobulin G), and four smaller proteins of similar size (lysozyme, ribonuclease, α-lactalbumin, and calcium depleted α-lactalbumin) were used at varying concentrations. The kinetics of the interfacial tension changes were described using a model accounting for diffusion-controlled adsorption of protein molecules and for conformational changes of already adsorbed molecules. Apart from the interfacial tension changes due to these two subprocesses, the model yields the diffusion relaxation time and the rate constant of the conformational changes. At low concentrations, adsorption of proteins did not always affect the interfacial tension, but its contribution to the decrease in interfacial tension increased with higher bulk concentrations. The decrease due to conformational changes remained a constant value for all proteins. The diffusion relaxation time could not be related to the diffusion coefficient of the protein, probably because of neglect of a reaction component in the model applied. Rate constants for conformational changes were generally lower at the solid–liquid interface, indicating that proteins are more apt to conformational changes at the liquid–vapor interface than at the solid–liquid interface. The least rigid protein, αLA($-Ca^{2+}$), had the largest rate constant for the conformational change at the two interfaces. © 1996 Academic Press, Inc.

Key Words: **FEP-Teflon; interfacial tension; protein adsorption; liquid–air interface; solid–liquid interface.**

INTRODUCTION

The surface active behavior of proteins is frequently employed in medicine and industry, as, for instance, in the development of new biomaterials, drug delivery systems, chromatographic separation, and the stabilization of emulsions and foams (1–4). The adsorption of proteins at an interface is accompanied by changes in the physical properties of the interface, particularly its interfacial tension γ.

[1] To whom correspondence should be addressed.

The change in interfacial tension is, among others, influenced by the protein bulk concentration and the molecular characteristics of the protein. Usually, at higher protein concentrations, a more rapid decrease of the interfacial tension is observed, together with a lower steady-state value (5, 6). Furthermore, relatively small, disordered proteins, like casein, will favor greater changes in interfacial tension than larger, globular and more stable proteins like albumin (6, 7). Paulsson and Dejmek (5) compared steady-state values of the interfacial tension caused by the adsorption of α-lactalbumin, β-lactoglobulin, and serum albumin at the liquid–air interface as reported by various groups. They concluded that there is a considerable spread in the results even under comparable conditions and that the rate of decrease of the interfacial tension is not a simple function of adsorption time and bulk concentration.

The change in the interfacial tension due to protein adsorption has frequently been derived from the Ward and Tordai equation (8),

$$\Gamma(t) = 2C_0\sqrt{\frac{Dt}{\pi}}, \qquad [1]$$

in which C_0 denotes the bulk concentration, D the diffusion coefficient, t the adsorption time, and $\Gamma(t)$ the surface protein concentration assuming that all molecules arrive at the surface by diffusion and adsorb irreversibly (perfect sink condition). Assuming that the decrease of the interfacial tension is a linear function of the number of segments adsorbed per molecule, ν, the interfacial pressure $\Pi(t)$ can be expressed as

$$\Pi(t) = \gamma(0) - \gamma(t) = 2\nu C_0 k_B T\sqrt{\frac{Dt}{\pi}}, \qquad [2]$$

$\gamma(0)$ being the initial interfacial tension, k_B the Boltzmann constant, and T the absolute temperature. A plot of $\gamma(t)$ vs $t^{1/2}$ will thus be linear at constant ν, and is frequently em-

0021-9797/96 $18.00

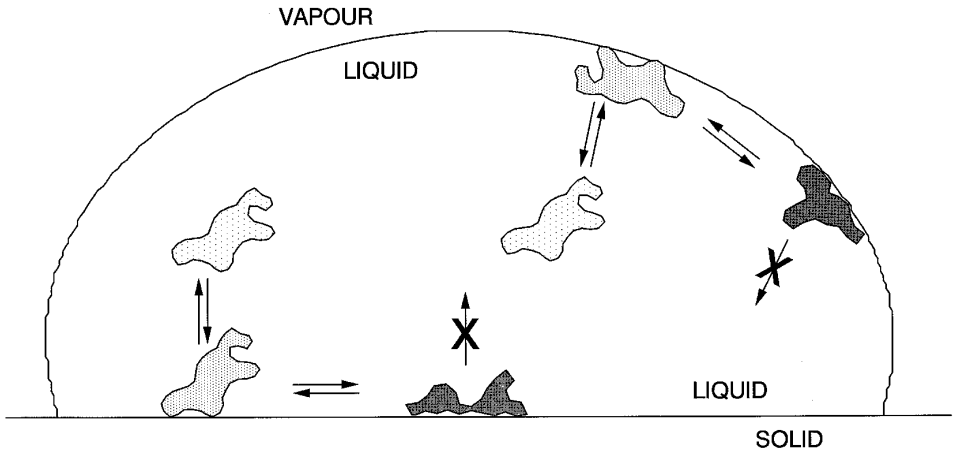

FIG. 1. In the adsorption model by Serrien *et al.* (14) as mathematically formulated by Eq. [3], proteins are assumed to diffuse toward an interface and adsorb barrierlessly. Subsequently, proteins may desorb or undergo conformational changes from their native state to adapt a state of minimal interfacial tension. Note that only proteins in their native, adsorbed state are assumed to be able to desorb.

ployed to designate different stages of the adsorption process (9–11).

The use of Eqs. [1] and [2] is justified as long as the interface acts as a sink. Consequently, linearity between γ and $t^{1/2}$ was only found at small concentrations or in the beginning of the adsorption process (9, 11–13). Also in the case of reversible adsorption Eq. [1] is still applicable for the initial stage of the adsorption process. With respect to adsorption kinetics, not only diffusion but also the actual interaction between the protein and the interface (denoted as ''the reaction component'') should be considered.

Serrien *et al.* (14) proposed a model which describes diffusion toward and subsequent reorientation and conformational changes at an interface by

$$\gamma(t) = \gamma(\infty) + \left\{\alpha \exp\left(-\sqrt{\frac{4t}{\pi\tau}}\right) + \beta\right\}\exp(-kt) \quad [3]$$

in which $\gamma(\infty)$ is the interfacial tension in steady state, τ the diffusion relaxation time, and k the rate constant for the conformational changes at the interface. The total decrease $\gamma(0) - \gamma(\infty)$ is thought to be composed of a part α for diffusion-controlled adsorption, and a part β due to conformational changes of adsorbed proteins. Figure 1 schematically summarizes the events leading to the formulation of Eq. [3]. Equation [3] has performed satisfactorily for concentration dependent adsorption of BSA, casein, and buttermilk toward air–water and oil–water interfaces in pendant drops at the tip of a vertical capillary (14).

Most work on the surface active properties of the proteins has been done for the liquid–vapor interface, but these properties are similarly important for the solid–liquid interface. Recently, axisymmetric drop shape analysis by profile (ADSA-P) has been introduced to simultaneously study interfacial tension changes at both the liquid–vapor and the solid–liquid interfaces due to the adsorption of proteins from sessile droplets (15–17). It has been shown that the solid–liquid interfacial tension γ_{sl} decreases upon the adsorption of proteins in a concentration-dependent way for much longer times than required to reach stationary state adsorption, presumably due to ongoing conformational changes of adsorbed proteins.

The aim of this study is to simultaneously determine the kinetics of changes in the interfacial tensions of both liquid–vapor and solid–liquid interfaces during the adsorption of two large proteins (serum albumin and immunoglobulin G) and four smaller proteins (lysozyme, ribonuclease, and α-lactalbumin with and without its internal stabilizing calcium ion). For this purpose sessile droplets of protein solutions on fluoroethylenepropylene–Teflon were analyzed by ADSA-P.

MATERIALS AND METHODS

Proteins

The small globular proteins of similar molecular mass and shape used in this study are hen's egg lysozyme (LSZ, Sigma L-6876), bovine pancreatic ribonuclease A (RNase, Sigma R-5125), bovine milk α-lactalbumin (αLA, a gift from the Netherlands Institute of Dairy Science NIZO, Ede, The Netherlands), and calcium-depleted bovine milk α-lactalbumin (αLA($-Ca^{2+}$), Sigma L-6010). Furthermore, two proteins of greater size are used, namely bovine serum albumin (BSA, Sigma A-4503) and human immunoglobulin G (IgG, Sigma I-4506). Some of their physicochemical properties relevant to the adsorption process are given in Table 1. The

TABLE 1
Physicochemical Properties of the Proteins Employed Relevant to Their Diffusion and Adsorption to Interfaces

Property	LSZ	RNase	αLA	αLA(−Ca^{2+})	BSA	IgG
Molecular weight ($g \cdot mol^{-1}$)	14,600	13,680	14,200	14,200	67,000	169,000
Partial specific volume ($cm^3 \cdot g^{-1}$)	0.688	0.703	0.735		0.733	0.739
Dimensions (Å)	46 × 30 × 30	38 × 28 × 22	37 × 32 × 25	37 × 32 × 25	116 × 27 × 27	37 × 37 × 274
Diffusion coefficient ($cm^2 \cdot s^{-1}$)	10.4×10^{-7}	12.6×10^{-7}	10.6×10^{-7}		7.0×10^{-7}	4.0×10^{-7}
Isoelectric point (pH units)	11.1	9.4	4.3	4.3	4.7	5.8–7.3
Net charge at pH 7 (e)	7	5	−3	−5	−18	
Total hydrophobicity ($J \cdot g^{-1}$)	−7.6	−8.7	−5.8	−5.8	−3.8	
$T_{denaturation}$ (°C)	70	68	65	41	65	

Note. Data were obtained from Refs. (18–28).

proteins were used as received to prepare single protein solutions in potassium phosphate buffer (10 m*M*, pH 7.0) in a concentration range between 0.001 and 5 $mg \cdot ml^{-1}$.

Substratum

The solid surface used in this study was commercial grade fluoroethylenepropylene–Teflon, FEP–Teflon (Norton Fluorplast, The Netherlands). Surfaces were cleaned ultrasonically in ultra pure ethanol (99.0–100.0%; Merck, Germany) to yield water contact angles exceeding 106°.

Interfacial Tension Measurements

A 100 μl protein solution droplet was placed on the FEP–Teflon surface in an enclosed glass chamber (50 × 50 × 30 mm) containing a reservoir filled with slightly warmed water to prevent evaporation of water from the droplet. The

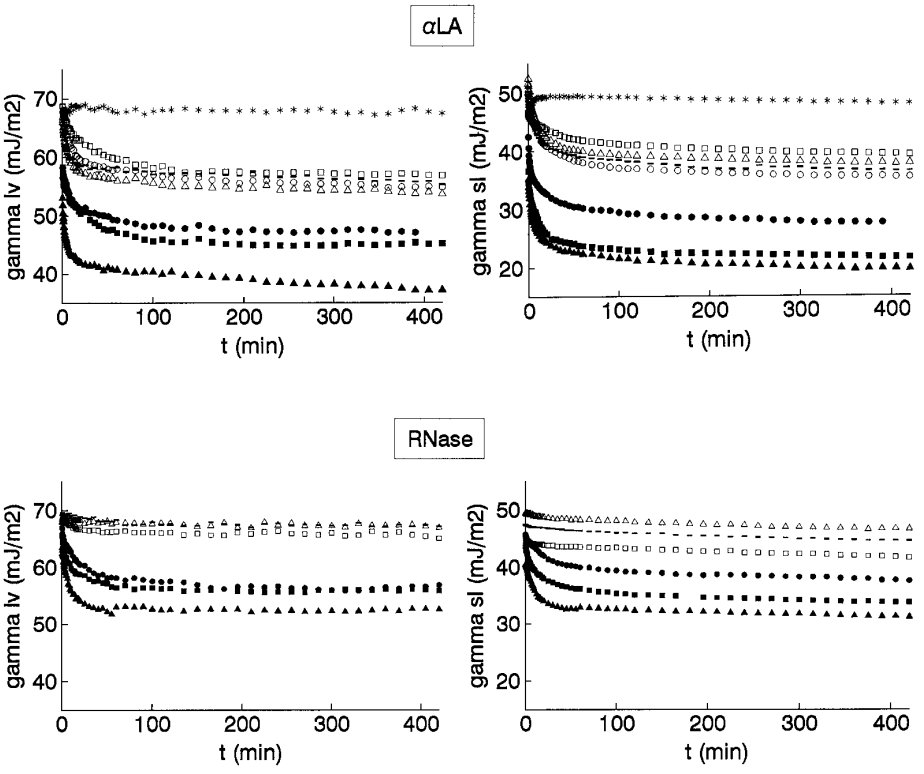

FIG. 2. Concentration dependence of the interfacial tension changes $\gamma_{lv}(t)$ and $\gamma_{sl}(t)$ for αLA and RNase solution droplets on FEP–Teflon as measured by ADSA-P. All data points are averages from three separate experiments with an approximate S.D. of 2 $mJ \cdot m^{-2}$ for the liquid–vapor and the solid–liquid interfaces. Symbols: (*) 0.001 $mg \cdot ml^{-1}$, (○) 0.005 $mg \cdot ml^{-1}$,(□) 0.01 $mg \cdot ml^{-1}$, (△) 0.05 $mg \cdot ml^{-1}$, (–) 0.1 $mg \cdot ml^{-1}$, (●) 0.5 $mg \cdot ml^{-1}$, (■) 1 $mg \cdot ml^{-1}$, (▲) 5 $mg \cdot ml^{-1}$.

TABLE 2
Induction Periods (min) for the Interfacial Tension Changes during the Adsorption of Different Proteins from Sessile Droplets on FEP–Teflon toward the Liquid–Vapor and the Solid–Liquid Interface

Concentration ($mg \cdot ml^{-}$)	0.001	0.005	0.01	0.05	0.1	0.5	1	5
				Liquid–vapor				
LSZ	>420	5	4	$3\frac{1}{2}$	2	0	0	0
RNase	[a]	[a]	>420	>420	>420	0	0	0
αLA	>420	$\frac{1}{2}$	1	$\frac{1}{2}$	0	0	0	0
αLA($-Ca^{2+}$)	>420	$3\frac{1}{2}$	1	0	0	0	0	0
BSA	>420	$9\frac{1}{2}$	4	$\frac{3}{4}$	0	0	0	0
IgG	>420	$\frac{1}{2}$	$1\frac{1}{2}$	10	$1\frac{1}{2}$	0	0	0
				Solid–liquid				
LSZ	>420	5	1	$3\frac{1}{2}$	1	0	0	0
RNase	[a]	[a]	>420	>420	>420	$1\frac{1}{2}$	0	0
αLA	>420	$\frac{1}{2}$	2	$\frac{1}{2}$	$\frac{1}{2}$	0	0	0
αLA($-Ca^{2+}$)	>420	$4\frac{1}{2}$	$1\frac{1}{2}$	0	0	0	0	0
BSA	>420	2	1	3	0	0	0	0
IgG	>420	$\frac{1}{2}$	$\frac{1}{2}$	12	1	0	0	0

Note. The values are rough estimates, and only visualize the presence and relative length of the induction period.
[a] Experiment not performed.

droplet profile was viewed with a video camera and its image digitized with a contour monitor as described earlier (29). The profile coordinates were used for calculation of the contact angle θ and the liquid surface tension γ_{lv} by axisymmetric drop shape analysis by profile, ADSA-P (30), making use of the relation between the liquid surface tension and the shape of a droplet as described by the Laplace equation. Measurements on one solution droplet were done as a function of time for at least 7 h at room temperature.

The major uncertainty in the experimental procedures involves the fact that $t = 0$ cannot be accurately determined since time is required to position the droplet and to focus and grab the image of the droplet profile. Therefore, in this study we considered the first image taken to represent $t =$ 5 s after the first contact between the droplet and the surface.

The results $\theta(t)$ and $\gamma_{lv}(t)$ were combined with the Young equation to yield the solid–liquid interfacial tension $\gamma_{sl}(t)$ at any time t during the adsorption process from

$$\gamma_{sl}(t) = \gamma_{sv} - \gamma_{lv}(t) \cdot \cos \theta(t), \qquad [4]$$

where γ_{sv} represents the solid–vapor interfacial tension. γ_{sv} was assumed to be 20 $mJ \cdot m^{-2}$ and not to change during the experiment (17).

This procedure was carried out three times with separate liquid droplets and data were averaged.

Analysis of the Kinetics

Equation [3] was used to fit the averaged data using the Levenberg–Marcquardt nonlinear parameter fitting routines offered by the MATHPAK 87 package (Precision Plus Software, Canada) to obtain relaxation constants τ for the diffusion-controlled decrease of the interfacial tension, rate constants k for the conformational changes at the interface, the equilibrium value $\gamma(\infty)$, and the corresponding components α and β of the interfacial pressure $\Pi(\infty)$. This analysis was carried out for the solid–liquid and the liquid–vapor interface, while setting $\gamma_{lv}(0)$ equal to the interfacial tension of the pure buffer (70 $mJ \cdot m^{-2}$) and $\gamma_{sl}(0)$ equal to 50 $mJ \cdot m^{-2}$, i.e., the interfacial tension between buffer and FEP–Teflon as measured by ADSA-P.

RESULTS

Figure 2 illustrates for αLA and RNase the concentration dependence of both the liquid–vapor and the solid–liquid interfacial tension, γ_{lv} and γ_{sl}, respectively, as a function of adsorption time t. The changes appear to be greatly dependent on the type of protein and the concentration, the greater changes being caused by the higher bulk concentration. The other proteins show similar concentration dependencies.

Sometimes the interfacial tensions $\gamma_{lv}(t)$ and $\gamma_{sl}(t)$ did not show the immediate decrease as a function of time and a so-called induction period was observed during which $\gamma(t)$ remained at its initial value. Table 2 summarizes the estimated induction periods for adsorption at the liquid–vapor and the solid–liquid interfaces. Generally, the induction period became smaller and finally disappeared upon increasing the protein concentration, except for IgG for which an in-

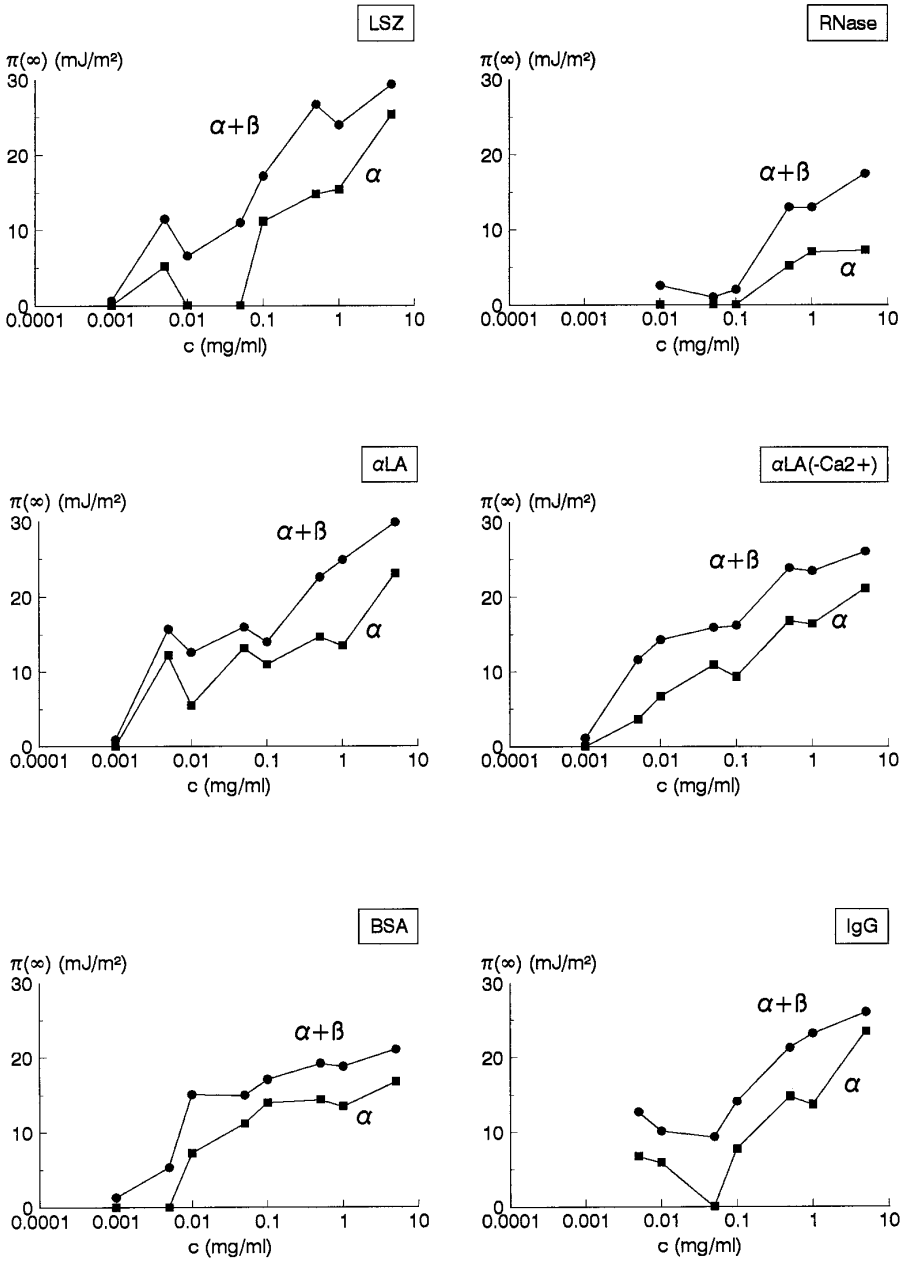

FIG. 3. Equilibrium interfacial pressure $\Pi(\infty)$ (denoted $\alpha + \beta$, ●) for adsorption of different proteins at the liquid–vapor interface and its components α (■) and β (difference) due to diffusion-controlled adsorption and conformational changes at the interface. α and β were obtained from a fitting procedure on an average curve for three separate experiments, yielding an uncertainty in α and β of 0.9 and 0.6 $mJ \cdot m^{-2}$, respectively, on an average. Note that for RNase at the lower concentrations, experiments were not done, while for IgG at $c = 0.001$ $mg \cdot ml^{-1}$ no convergence of the fit could be attained.

creased induction period was seen at 0.05 $mg \cdot ml^{-1}$ of about 10 min at the liquid–vapor interface, and of about 12 min at the solid–liquid interface.

Obviously, Eq. [3] is not suitable to fit the above type of kinetics. For this type of kinetics, Serrien *et al.* (14) suggested to modify Eq. [3] by assuming that during the induction period slow, diffusion-controlled adsorption does not contribute to the interfacial tension change, i.e., $\alpha = 0$ (14). Hence, Eq. [3] is assumed to reduce to

$$\gamma(t) = \gamma(\infty) + \beta \exp(-kt). \qquad [5]$$

The interfacial tensions $\gamma_{lv}(t)$ and $\gamma_{sl}(t)$ were used to fit Eq.

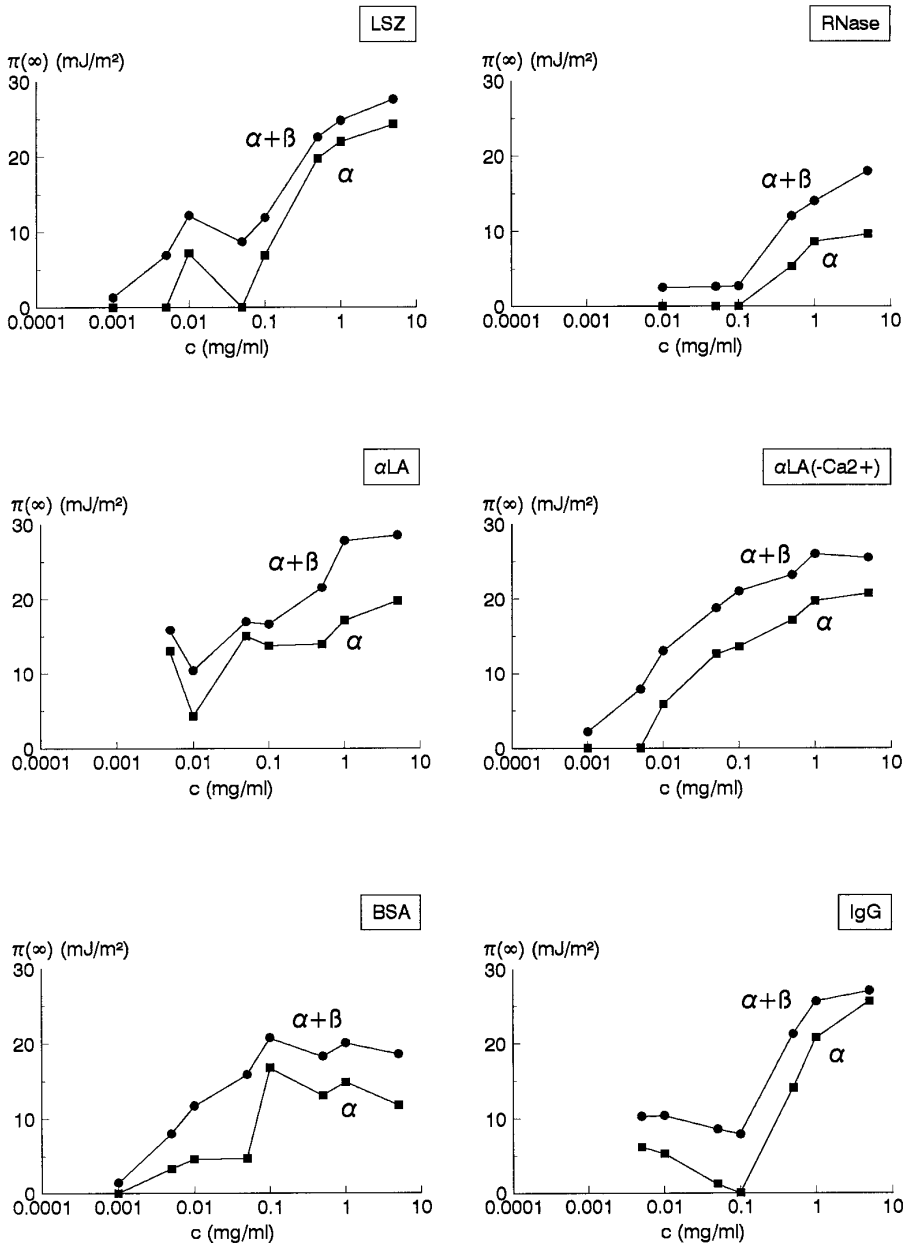

FIG. 4. Equilibrium interfacial pressure $\Pi(\infty)$ (denoted $\alpha + \beta$, ●) for adsorption of different proteins at the solid–liquid interface and its components α (■) and β (difference) due to diffusion-controlled adsorption and conformational changes at the interface. α and β were obtained from a fitting procedure on an average curve for three separate experiments, yielding an uncertainty in α and β of 0.9 and 0.6 $\mathrm{mJ \cdot m^{-2}}$, respectively, on an average. Note that for RNase at the lower concentrations, experiments were not done, while for IgG at $c = 0.001$ $\mathrm{mg \cdot ml^{-1}}$ no convergence of the fit could be attained.

[3] or [5] when appropriate to yield $\gamma(\infty)$, the components α and β, and the parameters τ and k.

In Figs. 3 and 4 the equilibrium interfacial pressures $\Pi(\infty)$ for the liquid–vapor and solid–liquid interfaces are presented together with their components α and β due to diffusion-controlled adsorption and conformational changes at the interface, respectively. The diffusion relaxation times τ and the rate constants k as resulting from these fits are summarized in Tables 3 and 4, respectively, for both the liquid–vapor and the solid–liquid interface.

DISCUSSION

Most techniques to study the surface tension γ_{lv} of protein solutions, like ring tensiometry, the Wilhelmy plate, or the capillary rise methods, neglect mass transport and

TABLE 3

Diffusion Relaxation Times τ (s) for Diffusion-Controlled Adsorption of Different Proteins from Sessile Droplets on FEP–Teflon toward the Liquid–Vapor and the Solid–Liquid Interface

Concentration ($mg \cdot ml^{-1}$)	0.001	0.005	0.01	0.05	0.1	0.5	1	5
				Liquid–vapor				
LSZ	[a]	136	[a]	[a]	632	5	17	4
RNase	[b]	[b]	[a]	[a]	[a]	48	77	1
αLA	[a]	582	430	336	152	3	2	28
αLA($-Ca^{2+}$)	[a]	212	27	106	99	2	2	2
BSA	[a]	[a]	937	573	355	10	11	3
IgG	[c]	122	136	[a]	772	374	34	181
				Solid–liquid				
LSZ	[a]	[a]	727	[a]	706	205	139	11
RNase	[b]	[b]	[a]	[a]	[a]	7	121	0.3
αLA	[c]	1103	20	790	754	34	4	19
αLA($-Ca^{2+}$)	[a]	[a]	21	628	443	20	15	24
BSA	[a]	319	544	20	465	424	29	228
IgG	[c]	308	704	14	[a]	381	288	433

Note. The diffusion relaxation times presented were obtained from a fitting procedure on an average curve for three separate experiments, yielding an uncertainty in τ of 40% on an average.

[a] Not calculated due to the use of Eq. [5].

[b] Experiment not performed.

[c] No satisfactory convergence of the fit could be attained.

adsorption of proteins to other interfaces than the liquid–vapor interface under study. Methods in which proteins are injected in the liquid phase may yield highly heterogeneous distribution of proteins, while stirring influences mass transport and hence the kinetics of the adsorption process (5, 31). Although it may be considered as an advantage of ADSA-P that protein adsorption can be studied simultaneously at both the liquid–vapor and the solid–liquid interface, transport conditions are complex especially during positioning of the protein solution droplet, which makes an

TABLE 4

Rate Constants k (10^{-3} s^{-1}) for the Conformational Changes during Adsorption of Different Proteins from Sessile Droplets on FEP–Teflon toward the Liquid–Vapor and the Solid–Liquid Interface

Concentration ($mg \cdot ml^{-1}$)	0.001	0.005	0.01	0.05	0.1	0.5	1	5
LSZ	0.1[a]	0.1	0.3[a]	0.4[a]	0.2	1.3	1.8	1.0
RNase	[b]	[b]	1.0[a]	0.2[a]	0.4[a]	0.5	0.6	1.8
αLA	0.1[a]	0.1	0.3	0.1	0.1	0.5	0.6	0.1
αLA($-Ca^{2+}$)	0.1[a]	0.2	0.2	0.2	0.2	2.5	2.4	2.1
BSA	0.5[a]	0.2[a]	0.1	0.1	0.1	0.7	0.3	0.2
IgG	[c]	0.1	0.1	0.2[a]	0.1	0.1	0.2	0.2
				Solid–liquid				
LSZ	0.5[a]	0.4[a]	0.1	0.2[a]	0.1	0.1	0.1	0.5
RNase	[b]	[b]	0.2[a]	0.1[a]	0.1[a]	0.3	0.2	1.2
αLA	[c]	0.1	0.2	0.1	0.1	0.3	0.8	0.4
αLA($-Ca^{2+}$)	0.1[a]	0.4[a]	0.2	0.1	0.1	0.5	0.7	0.4
BSA	1.0[a]	0.1	0.1	0.3	0.1	0.1	0.2	0.1
IgG	[c]	0.1	0.1	0.1	0.2[a]	0.1	0.1	0.1

Note. The rate constants presented were obtained from a fitting procedure on an average curve for three separate experiments, yielding an uncertainty in k of 20% on an average.

[a] Calculated by using Eq. [5].

[b] Experiment not performed.

[c] No satisfactory convergence of the fit could be attained.

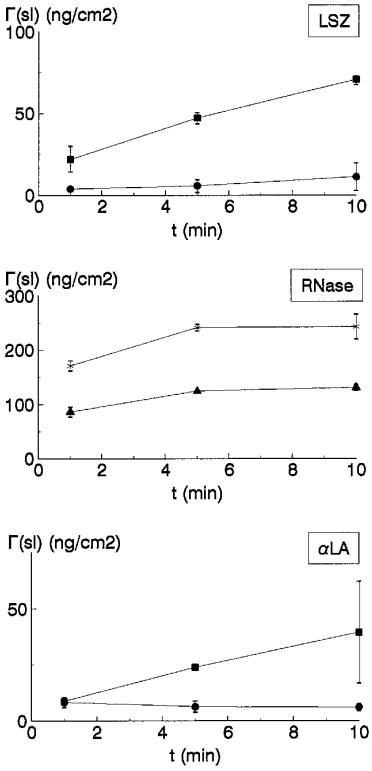

FIG. 5. Amounts of adsorbed protein at the solid–liquid interface (Γ_{sl}) as a function of time, obtained from adsorption experiments with similar 100 μl solution droplets on FEP–Teflon as in the ADSA-P measurements, while making use of iodinated LSZ, RNase, or αLA in 10 m*M* KPi, pH 7. For αLA($-Ca^{2+}$) no succesful iodination could be achieved. The bars indicate the standard deviations over three separate experiments. Data for BSA and IgG in 10 m*M* phosphate buffered saline, pH 7 have been published before (16, 17). Symbols: (●) 0.001 mg·ml^{-1}, (■) 0.005 mg·ml^{-1}, (▲) 0.01 mg·ml^{-1},(*) 0.05 mg·ml^{-1}.

analysis of the kinetics of interfacial tension changes at the interfaces highly complicated.

The model employed in this paper to analyze the kinetics of the interfacial tension changes has been used before by Serrien *et al.* (14) for single interface adsorption of albumin, casein, and buttermilk for pendant droplets and liquid–vapor interfaces which were continuously expanded or compressed. Although it was concluded that the model was suitable to describe the interfacial tension changes due to adsorption of these different proteins to the liquid–vapor interface, it is disturbing that, due to the nature of the experimental methods used, data were not consistent.

We found application of the model especially troublesome when a so-called induction period (see Table 2) occurred. Whereas others have simply shifted the time axis to eliminate this problem (14), we found this unacceptable as proteins were found to be present in the interface during the induction period (unpublished, see Fig. 5), and have chosen to use Eq. [5] in these cases, albeit that fitting remains difficult. Most likely, during the induction period, adsorbed proteins do not contribute to any change in interfacial tension until they have changed their conformation, which may sometimes take a relatively long time. Also, as interfacial tensions are related to surface excess concentrations rather than to absolute adsorbed amounts, the concentration ranges for which an appreciable induction period is seen may correspond with a situation in which the excess concentration of adsorbed proteins is zero. Consequently, the α part of the spreading pressure would be zero, but a nonzero spreading pressure may develop in time as a result of conformational changes. Note that as a result of this interpretation, negative surface excess concentrations at lower bulk protein concentration may be expected, possibly giving rise to negative interfacial tensions.

In an attempt to relate the relaxation time values to the diffusion coefficients of the proteins, data were fitted to

$$\tau = \frac{1}{D}\left(\frac{d\Gamma}{dC}\right)^2, \qquad [6]$$

in which Γ is the adsorbed amount of protein (14). Diffusion coefficients obtained were reasonable for IgG (1.6×10^{-7} cm^2 s^{-1}, compare Table 1) but were about 100-fold too small for BSA, and 20- and 10-fold too small for αLA and LSZ, respectively. For RNase, the analysis did not work at all. These differences are probably due to the fact that in Eq. [6], the reaction component is neglected, i.e., all repulsive interactions are assumed to be zero (''barrierless adsorption'') and all adsorbed proteins are assumed to be in a similar conformational state. Note that τ is larger at the solid–liquid interface than at the liquid–vapor interface (see Table 3), probably indicating that the influence of the reaction component is stronger at the solid–liquid interface than at the liquid–vapor interface. Tentatively, this could be due to the fact that stronger interacting forces arise from a high density medium than from a vapor phase.

With regard to the adsorption component α of the total interfacial pressure, it is noteworthy that the components α are greater at the higher than at the lower concentrations, while the least hydrophobic protein RNase has the smallest adsorption component. Regardless of hydrophobicity and hardness, the conformational components β, in a stationary endpoint of the adsorption process, are similar for all proteins, i.e., about 6 mJ·m^{-2}. The hardness of the proteins, as inferred from the denaturation temperature (see Table 1), is mostly reflected in the rate constant k for the conformational changes: k values for αLA are larger when the stability of the protein is decreased by the removal of its internal calcium ion (compare Tables 1 and 4). The stabilities of the other proteins probably do not differ enough to be reflected in the k values, even though they are generally higher

at the liquid–vapor than at the solid–liquid interface. It has been argued that, as a shortcoming of the model by Serrien *et al.* (14), Eq. [3] lacks a concentration term. It is our current interpretation that this criticism corresponds with the fact that the rate constants k, as found here, still demonstrate a concentration dependence.

Comparison of the present results with existing literature data is difficult, because variations in parameters such as pH, ionic strength, mass transport conditions, and protein concentration will have a major influence on the results. Nevertheless, our results for the spreading pressure of BSA at the liquid–vapor interface ($\pi\ (\infty) \sim 20\ \mathrm{mJ \cdot m^{-2}}$, maximally) correspond well with results of Graham and Phillips (32), reporting 17 $\mathrm{mJ \cdot m^{-2}}$ for BSA. For lysozyme, they (32) report an equilibrium spreading pressure of 15 $\mathrm{mJ \cdot m^{-2}}$, which is smaller than found here. There are few data available in the literature reporting an adsorption and conformation part of the spreading pressure. Serrien *et al.* (14) measured that the α part of the spreading pressures of BSA films on water varied from 9.5–14 $\mathrm{mJ \cdot m^{-2}}$ over the concentration range from 0.05 to 5 $\mathrm{mg \cdot ml^{-1}}$, similar to our findings, but their β part (8–12 $\mathrm{mJ \cdot m^{-2}}$) was higher. Large differences exist between the diffusion relaxation times τ and rate constants k presented here (Tables 3 and 4) and those of Serrien *et al.* (14), probably attesting to the influence of the above mentioned factors upon the results.

ACKNOWLEDGMENTS

The authors are greatly indebted to Professor P. Joos for his kind assistance in interpreting the data according to Eq. [3] and [5], and Dr. J. M. Meinders and J. Noordmans for writing the fitting program.

REFERENCES

1. Andrade, J. D., *in* ''Surface and Interfacial Aspects of Biomedical Polymers, Vol. 2: Protein Adsorption'' (J. D. Andrade, Ed.), p. 1. Plenum, New York, 1985.
2. Dickinson, E., *Food Hydrocolloids* **1,** 3 (1986).
3. Merritt, K., and Brown, S. A., *J. Biomed. Mater. Res.* **22,** 111 (1988).
4. Bonfield, T. L., Colton, E., and Anderson, J. M., *J. Biomed. Mater. Res.* **26,** 457 (1992).
5. Paulsson, M., and Dejmek, P., *J. Colloid Interface Sci.* **150,** 394 (1992).
6. Suttiprasit, P., Krisdhasima, V., and McGuire, J., *J. Colloid Interface Sci.* **154,** 316 (1992).
7. Evans, M. T. A., Mitchell, J., Mussellwhite, P. R., and Irons, L., *Adv. Exp. Med. Biol.* **7,** 122 (1970).
8. Ward, A. F. H., and Tordai, L., *J. Chem. Phys.* **14,** 453 (1946).
9. Benjamins, J., De Feijter, J. A., Evans, M. T. A., Graham, D. E., and Phillips, M. C., *Faraday Discuss.* **59,** 218 (1975).
10. Tornberg, E., *J. Colloid Interface Sci.* **64,** 391 (1978).
11. Song, K. B., and Damodaran, S., *Langmuir* **7,** 2737 (1991).
12. Bull, H. B., *J. Colloid Interface Sci.* **41,** 305 (1972).
13. Phillips, M. C., Evans, M. T. A., Graham, D. E., and Oldani, D., *Colloid Polym. Sci.* **253,** 424 (1975).
14. Serrien, G., Geeraerts, G., Ghosh, L., and Joos, P., *Colloids Surf.* **68,** 219 (1992).
15. Voigt, A., Thiel, O., Williams, D., Policova, Z., Zingg, W., and Neumann, A. W., *Colloids Surf.* **58,** 315 (1991).
16. Busscher, H. J. , Van der Vegt, W., Noordmans, J., Schakenraad, J. M., and Van der Mei, H. C., *Colloids Surf.* **58,** 229 (1991).
17. Van der Vegt, W., Van der Mei, H. C., and Busscher, H. J., *J. Colloid Interface Sci.* **156,** 129 (1993).
18. Haynes, C. A., and Norde, W., *Colloids Surf. B: Biointerfaces* **2,** 517 (1994).
19. Norde, W., and Anusiem, A. C. I., *Colloids Surf.* **66,** 73 (1992).
20. Norde, W., and Favier, J. P., *Colloids Surf.* **64,** 87 (1992).
21. Absolom, D. R., *in* ''Surface Characterization of Biomaterials'' (B. D. Ratner, Ed.), p. 101. Elsevier, Amsterdam, 1988.
22. Arai, J., and Norde, W., *Colloids Surf.* **51,** 1 (1990).
23. Peters, Th., Jr., *Adv. Prot. Chem.* **37,** 161 (1985).
24. ''CRC Handbook of Biochemistry—Selected Data for Molecular Biologie'' (H. A. Sober, Ed.), 2nd ed. CRC Press, Cleveland, 1973.
25. Johnson, J. E., and Matijević, E., *Colloid Polym. Sci.* **270,** 353 (1992).
26. Norde, W., and Lyklema, J., *J. Colloid Interface Sci.* **66,** 257 (1978).
27. Wahlgren, M. C., Paulsson, M. A., and Arnebrant, T., *Colloids Surf. A: Physicochem. Eng. Aspects* **70,** 139 (1993).
28. Tripp, B. C., Ph. D. Thesis, p. 28, Dep. of Chem. Fuels Eng., University of Utah, 1993.
29. Noordmans, J., and Busscher, H. J., *Colloids Surf.* **58,** 239 (1991).
30. Rotenberg, Y., Boruvka, L., and Neumann, A. W., *J. Colloid Interface Sci.* **93,** 169 (1983).
31. Subirade, M., Gueguen, J., and Schwenke, K. D., *J. Colloid Interface Sci.* **152,** 442 (1992).
32. Graham, D. E., and Phillips, M. C., *J. Colloid Interface Sci.* **70,** 415 (1979).